*35th EPS Conference on Plasma Phys. Hersonissos, 9 - 13 June 2008 ECA Vol.**32D**, P-2.037 (2008)*

Radial transport in the L- and H-mode SOL of ASDEX Upgrade

F. Mehlmann[1], C. Ionita[1], H.W. Müller[2], P. Balan[1], A. Herrmann[2], A. Kendl[1], M. Maraschek[2], V. Naulin[3], A.H. Nielsen[3], J. Juul Rasmussen[3], V. Rohde[2], R. Schrittwieser[1], and the ASDEX Upgrade Team[2]

[1]*Institute for Ion Physics and Applied Physics, Association EURATOM-ÖAW, University of Innsbruck, A-6020 Innsbruck, Austria*
[2]*Max-Planck-Institute for Plasma Physics, EURATOM Association, D-85748 Garching, Germany*
[3]*Association EURATOM - Risø DTU, Technical University of Denmark, DK-4000 Roskilde, Denmark*

Abstract: The radial turbulent particle flux in the scrape-off layer (SOL) in ASDEX Upgrade was investigated. A reciprocating probe was used with a probe head containing five Langmuir probes with which the poloidal and radial electric field fluctuations and those of the density were determined. A statistical analysis of the radial particle flux is presented for L-mode and H-mode shots. In the H-mode case, the intervals during type-I ELM events and during the ELM-free periods are analysed. Under certain conditions the transport during the L-mode in the SOL appears to be larger than during the ELM-free periods of the H-mode.

It is a well established fact that the radial turbulent flux in the plasma edge region of a magnetically confined toroidal plasma is mainly due to electrostatic fluctuations and carried by the fluctuating radial $E\times B$ drift. In the present paper we analyze the fluctuation-driven flux both in L-mode and H-mode discharges in ASDEX Upgrade (AUG). During the H-mode we have compared the periods during ELMs and in between ELMs.

A probe head with five carbon fibre composite pins (each 1 mm diameter and 3 mm length) was mounted inside a case of the same material. The probes are isolated from the case and from each other by boron nitride (see Fig. 1) [1]. As seen from the plasma, three pins (*ul* – upper left, *ll* – lower left and *m* – middle) measure the respective floating potentials V_{fl}. One probe (*ur* – upper right) is biased to –70 V to measure the ion saturation current I_{sat}. The fifth probe is swept to record the current-voltage characteristic. The poloidal spacing between the probes *ul* and *ll* is d_p = 5 mm. Probe *m* is radially protruding by d_r = 5 mm from the plane of the other probes.

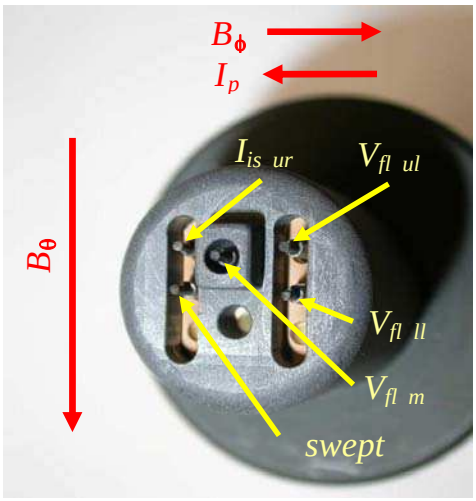

Fig. 1: Photography of the probe head as seen from the plasma, mounted on the midplane manipulator of ASDEX Upgrade.

This probe head was mounted on the fast reciprocating probe shaft of the AUG mid-plane manipulator and inserted up to four times into the scrape-off layer (SOL) during an AUG discharge. Typically a shot had a duration of up to 7 s. The window for signal evaluation during each stroke was 80 ms while the probe was on a stationary position. This probe arrangement allows the determination of the instantaneous radial fluctuation-induced particle flux density Γ_r

$$\Gamma_r = \tilde{n}_i \tilde{v}_r = \frac{\tilde{n}_i \tilde{E}_\theta}{B_\phi} \cong \frac{\tilde{n}_i \left(\tilde{V}_{fl\_ll} - \tilde{V}_{fl\_ul} \right)}{d_p B}, \qquad (1)$$

with n_i being the ion density, derived from the ion saturation current. $E_\theta \cong \left(\tilde{V}_{fl\_ll} - \tilde{V}_{fl\_ul} \right) / d_p$ is the poloidal electric field and B_ϕ the toroidal magnetic field, approximated by the total magnetic field B. From this also the averaged flux density $\langle \Gamma_r \rangle = \int_{t_0}^{t_1} \Gamma_r \, \mathrm{d}t \Big/ (t_1 - t_0)$ can be calculated. Here we have assumed that the particle flux density is solely due to $E_\theta \times B_\phi$ drift [2]. For this procedure we have to presume that the electron temperature is equal on all three probe positions. During the insertions, the average radial protrusion of the probe pins towards the last closed flux surface with respect to the radial position of the ICRH limiter shadow was 5 cm. The distance from the LCFS was between 5 and 8 cm (see Table I).

Although we cannot make a direct comparison between L-mode and H-mode shots we point out that the global parameters during the AUG shots #20228 (H-mode) and #20233 and #20234 (L-modes at two different densities) were rather similar. This is shown in Table 1. An additional fact is that probe measurements show the local properties of the transport, whereas on a global scale the particle balance cannot be directly deduced from them.

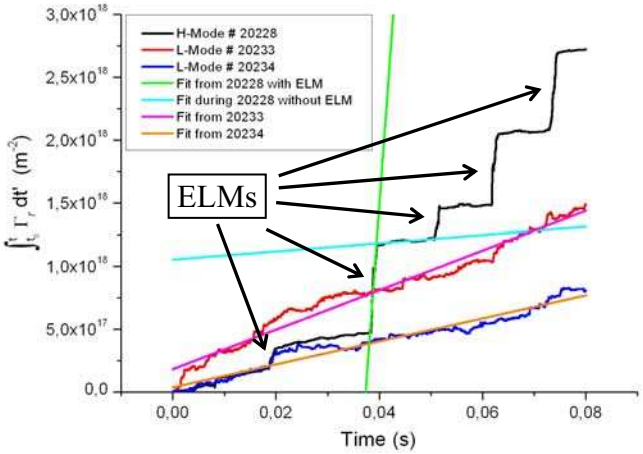

Fig. 2: Time integrated fluctuation-induced flux density with linear fits (thin straight lines) of the slopes for the L-mode shots (red and blue) and during the H-mode shot (black).

Fig. 2 demonstrates the development of turbulent transport with the time for the three above mentioned cases by the integral $\int_{t_0=0}^{t} \Gamma_r \, \mathrm{d}t'$. The fitted slopes of these curves are a good visualization of the averaged flux density during the shots. The red and blue curve and their linear regressions (straight lines) show that the flux density is more or less constant during the L-mode shots. The black

curve shows the strong difference between the transport during ELM events and during "inter-ELM" intervals. Therefore the straight lines are much steeper in the former cases than in the latter ones. Table I shows the values of the slopes, i.e., the averaged flux densities for the two L-mode shots #20233 and #20234 and the H-mode shot #20228 (in this case during four accumulated ELMs and during the periods in between ELMs), together with the global parameters of the shots and the distances from the LCFS.

Table I. Slope of the linear fits, showing the average fluxes, and global shot parameters (the symbols have their usual meaning)

Shot number, evaluated interval	$\langle\Gamma_r\rangle$ ($m^{-2}s^{-1}$)	I_p (MA)	B_t (T)	n_e (m^{-3})	NBI (MW)	Distance to LCFS (cm)
20228 H-mode, during ELMs	$5{,}6\times10^{20}$	1,005	–2,486	$9{,}0\times10^{19}$	5,2	5
20228 H-mode, in between ELMs	$3{,}2\times10^{18}$	1,005	–2,486	$9{,}0\times10^{19}$	5,2	5
20233 L-mode	$1{,}6\times10^{19}$	1,007	–2,494	$7{,}8\times10^{19}$	5,2	8
20234 L-mode	$9{,}1\times10^{18}$	1,007	–2,496	$8{,}5\times10^{19}$	5,2	8

The average flux density during ELMs is about 175 times larger than during inter-ELM times and about 35 times larger than during shot #20233 and 61 times larger than during shot #20234, respectively. The flux density during these L-mode shots is about 5 respectively 3 times larger than during inter-ELM intervals. Thus we arrive at the conclusion that the locally measured particle flux density is larger in the H-mode than in the L-mode shots. In addition, we discern that in spite of the higher density in shot #20234 the flux density is lower than in shot #20233.

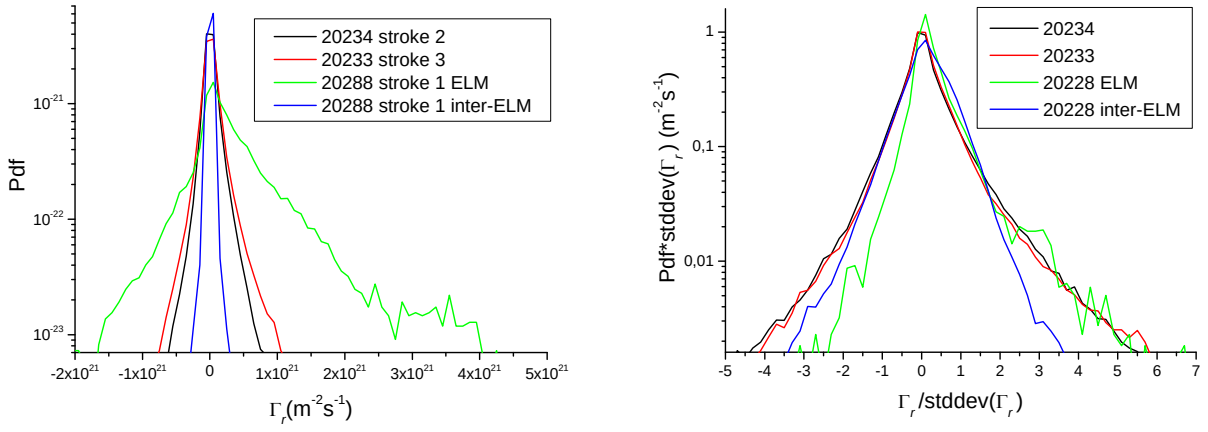

(a) (b)

Fig. 3: (a) Pdfs of the radial fluctuation-induced particle flux density comparing periods during ELMs (green line), inter-ELM intervals (blue line) and L-modes (black and red line); (b) same rescaled to the standard deviations.

For obtaining a better comparison between the four cases, Fig. 3 shows the probability density functions (pdf) of the flux density Γ_r (Fig. 3a) and the rescaled pdfs of $\Gamma_{norm} = \Gamma_r/\mathrm{stddev}(\Gamma_r)$ (Fig. 3b), the latter being normalized to their specific standard deviations (stddev). The pdfs in Fig. 3a show the strong difference of the flux densities in the four cases and the predominately outward transport in the SOL during ELMs (green pdf) [3]. On the other hand, the blue pdf is the narrowest and most symmetric showing the small transport and good confinement in between ELMs compared to the two L-mode pdfs (black and red). In Fig. 3b most remarkable is that the right-hand side flanks of the pdfs and their skewnesses are nearly the same during ELMs (green line) and during the L-mode shots (black and red lines). These results corroborate the conclusion that in the H-mode the ELMy transport during the ELM intervals shows qualitatively similar statistical characteristics as for the transport in the L-mode, where the transport is known to be mediated by radially propagating blob structures [4,5]. On the other hand, during the inter-ELM intervals our local probe measurements show no strong events and diffusive transport dominates.

Acknowledgements

This work, supported by the European Communities under the Contracts of Associations between EURATOM and the Austrian Academy of Sciences, the Max-Planck Institute for Plasma Physics and RISØ was carried out within the framework of the European Fusion Development Agreement. The content of the publication is the sole responsibility of its authors and it does not necessarily represent the views of the Commission or its services. This work was also supported by projects P14545 and L302-N02 of the Austrian Science Fund.

References

[1] P. Balan, V. Naulin, J.J. Rasmussen, A. Kendl, C. Ionita, R. Schrittwieser, A. Herrmann, M. Maraschek, H.W. Müller, V. Rohde, ASDEX Upgrade Team, Europhys. Conf. Abst. 30I, P-2.128 (2006).

[2] P.C. Stangeby, A.V. Chankin, Nucl. Fusion 36, 839 (1966).

[3] B. Nold, M. Maraschek, H.W. Müller, M. Ramisch, V. Rohde, U. Stroth, the ASDEX Upgrade Team, contribution to this conference.

[4] O.E. Garcia, J. Horacek, R.A. Pitts, A.H. Nielsen, W. Fundamenski, J.P. Graves, V. Naulin, J. Juul Rasmussen, Plasma Phys. Control. Fusion 48, L1-L10 (2006).

[5] A. Kirk, B. Koch, R. Scannell, H. R. Wilson, G. Counsell, J. Dowling, A. Herrmann, R. Martin, M. Walsh, MAST team, Phys. Rev. Lett. 96, 185001 (2006).